**EVENS ROBERT**

# IMPACTS OF LAND USE ON WATER INFILTRATION IN VARIOUS SOILS OF THE CANTAREIRA SYSTEM

**LAVRAS – MG**

**2021**

**EVENS ROBERT**

# IMPACTS OF LAND USE ON WATER INFILTRATION IN VARIOUS SOILS OF THE CANTAREIRA SYSTEM

Thesis presented to the Federal University of Lavras, as part of the requirements of the Graduate Program of Soil Science, concentration area of the Environmental Resources and Land Use, to obtain the title of Master in Soil Science.

Prof. Dr. Junior Cesar Avanzi
Advisor
Prof. Dr. Bruno Montoani Silva
Co-advisor

**LAVRAS – MG**

**2021**

**Ficha catalográfica elaborada pelo Sistema de Geração de Ficha Catalográfica da Biblioteca Universitária da UFLA, com dados informados pelo(a) próprio(a) autor(a).**

Robert, Evens.
Impacts of land use on water infiltration in various soils of the Cantareira System / Evens Robert. - 2021.
57 p. : il.

Orientador(a): Junior César Avanzi.
Coorientador(a): Bruno Montoani Silva.
Dissertação (mestrado acadêmico) - Universidade Federal de Lavras, 2021.
Bibliografia.

1. Infiltration rate. 2. Land use. 3. Soil classes. I. Avanzi, Junior César. II. Silva, Bruno Montoani. III. Título.

**EVENS ROBERT**

# GROUNDWATER RECHARGE POTENTIAL AS AFFECTED BY SOIL PROPERTIES AND LAND USE IN THE CANTAREIRA SYSTEM

Thesis presented to the Federal University of Lavras, as part of the requirements of the Graduate Program of Soil Science, concentration area of the Environmental Resources and Land Use, to obtain the title of Master in Soil Science.

APPROVED in: April 26th of 2021.

Dr. Bruno Montoani Silva UFLA

Dr. Salvador Francisco Acuña-Guzman UFLA

Dr. Eduardo da Costa Severiano IF GOIANO

Prof. Dr. Junior Cesar Avanzi

Advisor

**LAVRAS – MG**

**2021**

# ACKNOWLEDGEMENTS

I thank God for preserving my health and protecting me during these two years while I worked on my research program.

I thank my parents, Nodith Chery, who gave me her constant support and encouragement in spite of the stress and loneliness she sometimes felt due to my absence; I thank her for her comfort and counsel which have greatly helped me and my Dad Eril Robert although he is not alive in my life, but his sacrifices mean a lot to me.

I thank my sisters, Ylanda Robert and Fabiolla Robert, who both encouraged me as well.

I thank University of Fondwa (UNIF), for the institution's help in providing me the base training and knowledge necessary to continue my academic career in Brazil.

I thank the Organization of American States (OAS) in partnership with CAPES for generously providing me this scholarship to study in Brazil and to obtain my master's degree in Soil Conservation and Water Management. This study was financed in part by the Coordenação de Aperfeiçoamento de Pessoal de Nível Superior – Brasil (CAPES) – Finance Code 001.

I thank the National Council for Scientific and Technological Development – CNPq for funding the research project (process 441244/2017-3).

I thank my advisor, Professor Junior Cesar Avanzi, for accepting and mentoring me, and for participating in this research study. His instruction and guidance have been indispensable to me during my master's program.

I thank my co-advisor, Professor Bruno Montoani Silva, who was always available to assist me whenever I needed by mentoring me on research and academic skills. I thank all of the professors at the Department of Soil Sciences at the Federal University of Lavras who helped me in one way or another, through teaching courses and transferring their knowledge with the utmost patience and devotion.

I thank my friend David Alexander Carroll II, who helped me tirelessly through teaching me about various subject, especially in science informatics, helping me develop the necessary base knowledge and skills to conduct data analyses. He also helped me by reviewing the translation of this document, and he assisted me in many other ways.

A special thanks to the love of my life Elayne Marques Silva for reviewing the entire document and providing her expertise as well.

Thanks also to my other colleagues such as Monna Lysa Teixeira Santana, Fernandes, Raphael, Wharley Pereira, Dany Guim, and Dione, for all of the support they gave me during this study program.

“Pour mériter l’estime, il n’est pas indispensable d’avoir fait de grandes choses, il suffit de les avoir tentées.”

Edgar La Selve

# ABSTRACT

The groundwater recharge depends on deep drainage. For this to occur, initially there must be infiltration of water into the soil. The soil use and management strong influence the process of water infiltration. In Cantareira System, the knowledge of soil classes combined with the land use is an essential for indicate the best use of the soil for each soil class, in order to promote an improvement in water recharge. The aim of this research was to determine the soil physical-hydric properties and the rate of basic infiltration in four different land uses under three soil classes. This research was carried out considering land uses of native forest, eucalyptus, rotated grazing and continuous grazing which occur in Red Yellow Argisols, Haplic Cambisols, and Regolith Neosols in the Cantareira System. Soil physical properties determined in laboratory were texture, bulk density, micro and macro porosity, total porosity, and soil aggregates. Soil infiltration was determined by using a double ring infiltrometer and Horton model was performed to achieve the soil infiltration rate. The results were subjected to analysis of variance (ANOVA) and the means by Tukey's test (5% probability), and principal component analysis (PCA) was performed in the RStudio software. Cambisols revealed as having the highest infiltration rate under the use of native forest compared to other soils. For Neosols, the infiltration rate is almost the same, regardless of land uses. For Argisols, the rate of basic infiltration is higher under Eucalyptus compared to other uses. The native forest in Cambisols and neosols showed a higher rate of water infiltration compared to argisols and being an important area for preservation, strongly influencing the water recharge into the soil. Animal trampling may have caused compaction in continuous grazing, reflecting very low water infiltration values in the soils analyzed.



**Keywords:** Infiltration Rate. Horton model. Soil classes. Land use.

# RESUMO

A recarga das águas subterrâneas depende de uma drenagem profunda. Para que isso ocorra, inicialmente deve haver infiltração de água no solo. O uso e manejo do solo influenciam fortemente no processo de infiltração da água. No Sistema Cantareira, o conhecimento das classes de solo aliadas ao uso do solo é fundamental para indicar o melhor uso do solo para cada classe de solo, a fim de promover uma melhoria na recarga da água. O objetivo desta pesquisa foi determinar as propriedades físico-hídricas do solo e a taxa de infiltração básica em quatro diferentes usos do solo em três classes de solo. Esta pesquisa foi realizada considerando os usos do solo de floresta nativa, eucalipto, pastejo rotacionado e pastejo contínuo que ocorrem em Argissolos Vermelho Amarelo, Cambissolos Haplico e Neossolos Regolitos do Sistema Cantareira. As propriedades físicas do solo determinadas em laboratório foram textura, densidade do solo, micro e macro porosidade, porosidade total e agregados do solo. A infiltração do solo foi determinada por meio de um infiltrômetro de anel duplo e o modelo de Horton foi realizado para obter a taxa de infiltração do solo. Os resultados foram submetidos à análise de variância (ANOVA) e as médias pelo teste de Tukey (5% de probabilidade), e a análise de componentes principais (PCA) foi realizada no software RStudio. Cambissolos revelaram ter a maior taxa de infiltração sob uso de floresta nativa em comparação com outros solos. Para Neossolos, a taxa de infiltração é quase a mesma, independentemente dos usos do solo. Para Argissolos, a taxa de infiltração básica é maior sob o eucalipto em comparação com outros usos. A mata nativa dos Cambissolos e Neossolos apresentam maior taxa de infiltração de água em relação ao Argissolos e sendo uma importante área de preservação, influenciando fortemente na recarga da água para o solo. O pisoteio dos animais pode ter causado compactação em pastejo contínuo, refletindo valores de infiltração de água muito baixos nos solos analisados.

Palavras-chave: Taxa de infiltração. Modelo de Horton. Classes de solo. Uso da terra.

# LIST OF FIGURES

# LIST OF TABLES

# ACRONYMS

ANOVA – Analysis of Variance;

BD – Bulk Density;

BIR – Base Infiltration Rate;

CP – Continuous Pasture;

CX – Haplic Cambisol;

E – Eucalyptus;

GMD – Geometric Mean Diameter;

Macro – Macroporosity;

Micro – Microporosity;

NF – Native Forest;

PVA – Red Yellow Argisol;

RP – Rotative Pasture;

RR – Regolith Neosol;

TP – Total Porosity;

WMD – Weighted Mean Diameter.

# TABLES OF CONTENTS

# 1 INTRODUCTION

Water is one of the most highly demanded natural resources by human societies and natural ecosystems alike (Oki *et al*., 2006**)**. Water infiltration is a very important process in the hydrological cycle, for the recharge of aquifers because it is fundamental and for being affected by land use and management practices to the soils (Gaspard *et al*., 2007). Different factors can influence infiltration: mineralogy, texture, structure, initial humidity, porosity (Gaspard *et al*., 2007). The ability of water to infiltrate into the soil is considered a process in making the soil function, if at the land use management there is alteration of physical properties. The water infiltration capacity also allows good planning on the use and conservation of land management therefore that can recharge groundwater (Freitas, 2005). Groundwater recharge is defined as water infiltration rate which percolate in the water table of aquifer and constitute a reservoir of water for the underground water (Diodato and Ceccareli, 2006).

Aquifer recharge is the operation by which water infiltrates the soil through drainage wells, valleys (Jones and Banner, 2003). Different factors can condition aquifer recharge: Climate change, topography, soil, vegetation, and land use (Keese *et al*., 2005; Menezes *et al*., 2009) to be able to put in place a plan for the good use of land in the rural areas for a vast landscape that can be seen from all sides of the ecosystem. Soil physics attributes the way in which precipitation is distributed into runoff and water that enters the soil water balance, as well as the amount of water available to the soil. Among the factors that condition the recharge of the aquifer, some are linked to the physical attributes of the soil since the process of infiltration of water into the soil is a key element for the availability of water, in the event of erosion and at the level of the runoff that occurs and the recharge of the aquifer (Cecilio *et al*., 2003). Factors like climate, topography, soil class, land vegetation and land use related to aquifer recharge (Menezes *et al*., 2009) can also alter the recharge potential of aquifers (Arnold *et al*., 2000).

The Cantareira System is one of the largest water catchment systems on the planet with the capacity to supply nineteen million people in the metropolitan region of São Paulo and Minas Gerais with an area of approximately to 228,000 hectares covering twelve counties, and four of them in Minas Gerais (Atlas, 2017). In fact, it is essential to develop an understanding of pedological environments, as well as the major land use and management practices that occur in this region, as this will enable policymakers to understand how each soil type can best be used in an environmentally sustainable manner, in order to improve groundwater recharge.

Consequently, studies on soil water infiltration rate are very important as they can enable the development of policies to protect the environment and natural resources in the Cantareira system, and especially to combat erosion and promote healthy rates of groundwater recharge (Guerra, 2000).

Regarding this research, the use of a double ring infiltrometer was used to apply in infiltration models to evaluate four different methods of soil management, including: native forest, eucalyptus, pasture in rotation and continuous pasture, to identify which of these land use exhibits the highest potential of groundwater recharge in the region and identify constraints due to inadequate soil use and management in soils to degradation.

## 1.1 Objective

The main objective of this research was to determine the basic infiltration rate using the double ring infiltrometer method in four different land uses under three representative soil classes: Red Yellow Argisol, Haplic Cambisol, and Regolith Neosol in Cantareira System.

Specific objectives have also been pursued which are as followed:

- Evaluate the physical properties of the soils;
- Model the soil water infiltration rate curve;
- Calculate the final infiltration rate;
- Evaluate the groundwater recharge potential associated with each land use.

# 2 LITERATURE REVIEW

## 2.1 Characterization of the experimental area

In the southern part of the State of Minas Gerais and the northwest of the State of São Paulo, the Cantareira System is a large complex of reservoirs used to store potable water for the São Paulo metropolitan region – the biggest urban agglomeration in South America (Whately and Cunha, 2007) with 19 million of people covers approximately 227,803 hectares of land (2,278.0 km²) and is in 12 municipalities, being four in Minas Gerais (Camanducaia, Extrema, Itapeva and Sapucaí-Mirim) and eight in São Paulo (Bragança Paulista, Caieiras, Franco da Rocha, Joanópolis, Nazaré Paulista, Mairiporã, Piracaia and Vargem). About 55% of the Cantareira System is located in the State of São Paulo and 45% in the State of Minas Gerais (Atlas, 2017). This system is made up of a series of reservoirs that hold water for public municipal use in the cities and communities located in the watersheds of the Tietê and Piracicaba Rivers (Ana, 2014).

Figure 1 – Municipalities that are part of the Cantareira System.

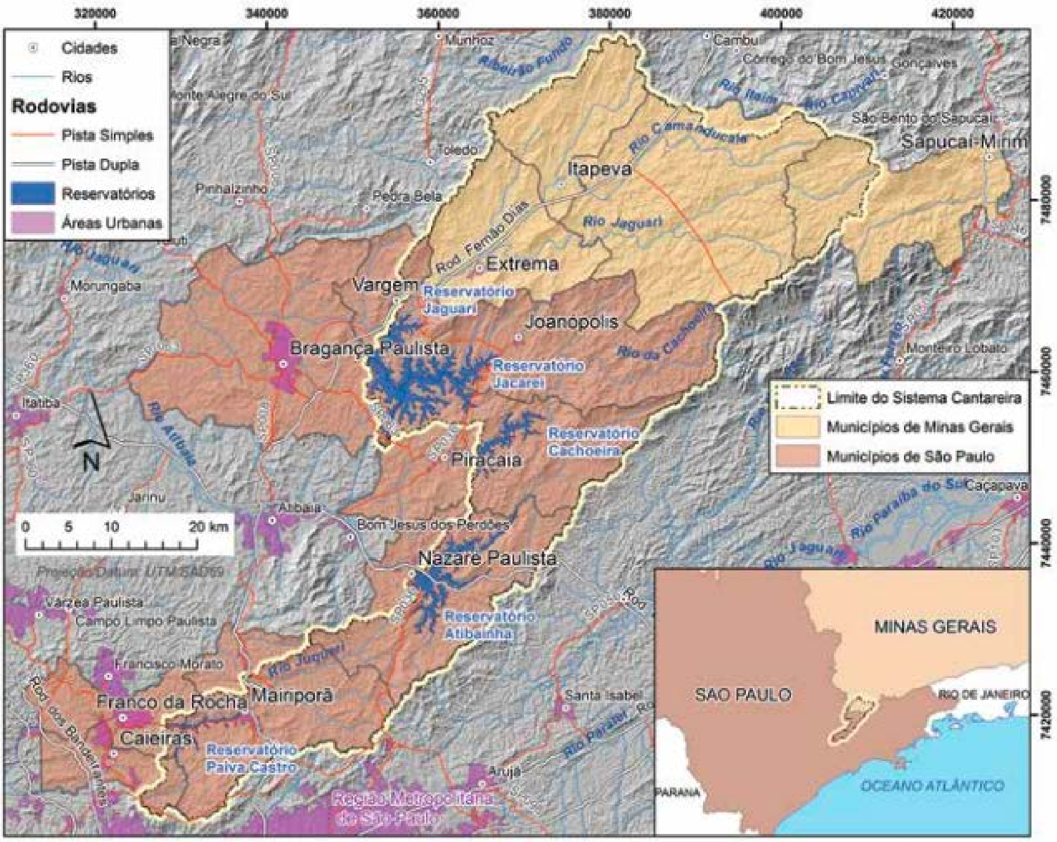


Source: IBGE (2006).

## 2.2 Climate

The climate is subtropical, cold in April and rainy in October with annual average temperatures ranging from a low of 18 ºC to a high of 20 ºC, the average annual rainfall is 1,570 mm. Between the years 2013 and 2015 the Cantareira System suffered the biggest supply crisis in its history, due to a decrease in rainfall in the region in that period. Between August 2013 and July 2015, the accumulated precipitation was 2,116 mm, about 67% of what was expected according to the historical average (3,143 mm). Approximately 40% of the Cantareira region is still covered by Atlantic Forests, although native vegetative communities are highly fragmented by agricultural land use. Pastures for cattle and eucalyptus plantations are the dominant agricultural activities in terms of land area, although some municipalities also have significant land area planted in vegetable and seed production plots (Atlas, 2017).

## 2.3 Soils

According to Freitas *et al*. (2008), the area of the Cantareira System is well known by three (3) predominant types of soil; 31.7% of the sub basin area is Red Yellow Argisol, 41.2% represented by Haplic Cambisol, 27.1% is Regolith Neosol.

## 2.4 Water infiltration process in the soil

Water infiltration in the soil is the process by which water vertically penetrates the soil surface (Brandão *et al*., 2006). According to Carvalho and Silva (2006), infiltration is a process that depends on several factors such as land condition, soil type, soil moisture, vegetation cover, soil compaction by machines and / or animals. The water infiltration rate into the soil is high at beginning of the infiltration process, when the soil is initially very dry, but tends to decrease over time. Therefore, under heavy rain or irrigation, the infiltration rate gradually approaches a minimum and constant value, called final or stable infiltration rate. Water infiltration data are important in different models used to describe water infiltration into the soil and depend on the area caused by the impact of raindrops on the soil surface (Alves Sobrinho *et al*., 2003). Knowledge of the process of water infiltration into the soil is of great importance in the management of soil conservation, hydrology, in irrigation projects, as well as in agricultural production. The damage caused by changes in water infiltration in the soil and subsoil, due to the gradual waterproofing process, whether by natural factors or by human activity, is immeasurable.

## 2.5 Infiltration models

To facilitate good management of irrigation systems and the use of water resources, some authors have come up with theoretical and empirical mathematical models in different infiltration models (Sihag *et al*., 2017). Theoretical models are more complex because they are based on physical flow theories and require a larger number of input parameters. The empirical models are simpler, and their parameters are estimated from the regression curve fitted to the infiltration values collected in the field. Among the empirical models, the most used are those of Kostiakov, Horton, Kostiakov-Lewis, and Philip (Almeida *et al*., 2014).

The model of Kostiakov do not consider the initial soil moisture. And using a *log I* versus *log T (k)* and *log T* (n) graph, the model of the Kostiakov equation is defined as a practical empirical model with which we can estimate parameters like the data of accumulated infiltration ($A_i$) as a function of time. Therefore, the average moisture content in the soil must be considered to perform the infiltration test (Fonseca and Duarte, 2006). As for the Kostiakov-Lewis, infiltration tends toward the final infiltration rate used mainly in the field of irrigation to estimate the accumulated infiltration (Teixeira *et al*., 2010). With the intensity of the low precipitation, to predict the rate of soil water infiltration as the infiltration rate exceeds the initial infiltration rate of the soil, the application of Horton should be applied. The Horton equation describes the factors related to soil surface such as the phenomena of soil expansion which aims to control the reduction in the infiltration rate over time, it is an exponential function (Prevedello, 1996). This model is estimated by linear regression in the field from the infiltration data by theorical equations.

## 2.6 Effects of soil type on infiltration

Infiltration capacity varies across soil class, organic matter content, and texture. For example, the relative proportion of sand, silt, and clay in a soil affects the size and number of pores as well as the water holding capacity of the soil (Klein *et al*., 2002). As an example of this, a study of no-till agricultural systems in the Conceição River catchment, located in the northwest portion of the State of Rio Grande do Sul, Brazil, revealed that there were significant problems associated with surface runoff and sediment yield; this is despite the fact that one of the objectives of no-till cultivation is to reduce erosion. Many areas in the watershed had soil loss rates higher than those considered acceptable for the region and the tillage system; this could be due to improper soil management and high soil compaction, which resulted in low soil water infiltration rates (Didoné *et al*., 2015).

Water infiltrates much more rapidly into sandy soils as compared to soils with higher silt and especially clay content; this is because sandy soils have larger pore spaces and a sufficient level of aggregation, which enables rapid movement of water into the soil profile (Bernardo *et al*., 2006). In Haplic Cambisol which have a beginning level of formation and relatively poorly developed soil profiles, soil water infiltration is facilitated by the high level of sand content and mineral aggregation (Soares *et al*., 2008). In the majority of Cambisols, average infiltration rates of between 300- and 400-mm $h^{-1}$ have been observed (Silva *et al*., 2006). After episodes of intense precipitation such as heavy rainfall, values from 63 to 75 mm $h^{-1}$ have been observed in various soil types and land management scenarios (Mariotti, 2013).

Red Yellow Argisol conversely, are characterized by high levels of iron and clay-rich subsoil horizons and are often associated with tropical areas of Brazil and other tropical countries. Although water may infiltrate less rapidly into argisols as compared to Haplic Cambisol, the water holding capacity of these soils is higher, given the clay-rich subsoil (Reichardt, 1987).

An analysis of Red Yellow Argisol reveals that the soil profile is often much deeper than other taxonomy classes, and that these soils are well-structured and well-drained. Water infiltration rates have been described as significant (15 - 30 mm $h^{-1}$), according to the classification system suggested by Reichardt (1987), because of its sufficient sand content. This is despite the relatively high density and low porosity of Red Argisols.

The final infiltration rate was determined in a Red Yellow Argisol under various management conditions, and the base infiltration rate was found to be 41% lower in tilled soils as compared to undisturbed soils (Alves and Cabeda, 1999). When measuring the base infiltration rate using double ring infiltrometers, subjected to minimum levels of crop management, both with and without conventional tillage, it was found base infiltration rate values were associated with minimum levels of crop management, and values were lower in soils that had not been tilled (Alves and Cabeda, 1999).

With an average depth of 0.5 m, the Regolithic Neosol are soils in which the A horizon covers the C horizon, with low levels of organic matter, low water retention, and with a content of easily alterable mineral content of 4% or greater in sand fraction (Embrapa, 2013). In Regolithic Neosols with semi-sandy texture, high bulk density, low macroporosity, and high microporosity, the cumulative infiltration rate is estimated at between 164 mm $h^{-1}$ and 136 mm $h^{-1}$ (Araujo *et al*., 2013), while analyzing the profiles of Neosols originating in volcanic rocks, average infiltration rate of between 347 mm $h^{-1}$ and 556 mm $h^{-1}$ was observed under the same parameters (Stürmer *et al*., 2009).

## 2.7 Effects of land use and management on infiltration

Soil management plays an important role in health of the soil surface and affects soil physical properties such as bulk density, porosity, organic matter content, aggregate stability, and soil water infiltration rate (Pinheiro *et al*., 2009). These properties have a significant impact on water infiltration and runoff processes and the interplay between these processes (Price *et al*., 2010). Factors such as soil class and soil management have an effect on velocity of raindrops hitting the soil surface, infiltration rates, runoff, and erosion (Silva, 2016).

In Brazil, water infiltration in forest environments is estimated to occur at a rate between 2 and 15 times higher than in agricultural lands, because high permanent vegetative cover significantly increases water infiltration capacity. Permanent vegetative cover improves soil physical properties, increases the porosity and aggregate structure of the soil, and facilitates a higher rate of infiltration (Espindola, 2004). Infiltration rates are lower in other land use types and vegetative communities in comparison to soils under forest (Lawall *et al*., 2009). Water infiltration occurs faster through soil profiles when vegetative cover is high because vegetation protects the soil surface from the direct impact of raindrops during precipitation events, and it also reduces runoff on the soil surface and water erosion (Araujo *et al*., 2013).

Vegetative cover reinforces positive soil physical properties through increasing the porosity and the soil aggregation, which contributes to improving soil water infiltration (Espindola, 2004). In a study conducted by Bono (2012), with native vegetation, soil water infiltration was stable over a period of seven years.

Soil water infiltration rate is a parameter that is reflected in the capacity of water to move through the soil, which enables researchers to determine the state of soil degradation (Gondim *et al*., 2010). Vegetative cover, which facilitates greater water infiltration, is very important to groundwater recharging processes and enables important hydrological processes to function properly (Almeida *et al*., 2012).

A study of soil erosion processes and trends along Cravo Stream in Nazareno, Minas Gerais, Brazil revealed that well-developed soils (in this case, Latosols), were more highly resistant to gully erosion than were soils with more weathered minerals such as granite-gneiss saprolite soils found in the area. In addition to soil class, land use also had a significant impact on soil erodibility (Sampaio *et al*., 2016). This suggests that processes in the Cantareira System associated with rural expansion, including expansion of grazing lands and croplands into native forest environment, is likely associated with increased soil erosion risk in general and increased gully formation in particular.

Study conducted on the Guaporé River Basin in southern Brazil found that there was little difference in soil erosion and runoff rates between forestland and cropland on gentle slopes, but that erosion was significantly higher on croplands than on forestlands on steep slopes (Vanacker *et al*., 2019); this suggests that there are significant interactions between topography and land use in determining soil erosion and water infiltration rates.

Study of soil runoff potential and the impact of land uses changes in Brazil revealed slightly different results; this study used the Soil and Water Assessment Tool (SWAT) model to evaluate the potential for increased or decreased soil water runoff when switching between forestland, pastureland, cropland, and bare soil in a watershed located in the Parque Estadual da Serra do Mar in Cunha Municipality, State of São Paulo. The SWAT model showed that changing land use from Atlantic Forest to cropland or pastureland (the process of rural expansion) would result in slight increases or decreases in runoff coefficients, but that the overall hydrological processes related to water infiltration versus runoff would not change significantly. The only land use that was associated with a significant decrease in soil water infiltration and an increase in runoff was bare soil (Lucas-Borja *et al.*, 2020; Anache *et al*., 2018).

Conducted a research in Itirapina, State of São Paulo with the Water Erosion Prediction Project (WEPP) model to analyze runoff and soil loss under various land management scenarios, calibrating the model with data from observed water runoff and soil loss from 2012 - 2016 in four land category types: wooded Cerrado forest, tilled fallow land without plant cover, pasture, and sugarcane. The results of the study showed that soil loss between wooded Cerrado and pasture were similar, suggesting that when using sustainable land management practices, pasturelands can mitigate some of the soil loss that could potentially come from expansion of human activities on forestlands. However, runoff rates were distinct between all four land use types, showing that runoff is higher on agricultural land than on forested land (Anache *et al*., 2018); since runoff is directly tied to infiltration, it can be inferred that forest cover promotes greater soil water infiltration than does anthropogenic land use types.

In general, a significant body of research exists examining the relationship between land use and soil health in Brazil, with specific focuses on runoff, soil moisture or water content, erosion potential, soil loss, and soil nutrient profiles. Many studies look specifically at the processes of anthropogenic land change that occur as forests are cleared for pastureland, crop cultivation, or development. While there is substantial research on land use change and soil physics in general, more information is needed on how soil water infiltration rates are influenced by various land use types in the region, as soil water infiltration is a significant component of overall soil moisture. This study addresses this knowledge gap by providing information on soil water infiltration rates across various land use types in the Cantareira System of Brazil.

# 3 HYPOTHESES

The hypotheses of this research are as follows:

- Considering the different soil classes that occur in the Cantareira System, native forest land cover will exhibit the highest rate of soil water infiltration.
- Pasture in rotation will exhibit the best overall soil quality index, which will contribute to a higher soil water infiltration rate and groundwater recharge potential when compared with continuous pasture.
- The soil water infiltration rate for soils under the eucalyptus land cover class will be lower than native forest, but higher than pasture in rotation or in continuous grazing.
- Considering the different soil classes, Haplic Cambisol will exhibit the highest rate of soil water infiltration regardless to other soil types mentioned in the research.

# 4 METHODOLOGY

## 4.1 Experimental design

This research was conducted in the municipalities of Nazaré Paulista, Piracaia, and Joanópolis (Figure 2), and on three different soil classes (Figure 3), including Red Yellow Argisol, Haplic Cambisol, and Regolith Neosol, according Brazilian Soil Classification System (Santos et al., 2018).

Each of these soil classes contained four different land use/ land cover categories namely native forest (NF), eucalyptus (E), pasture in rotation (PR), and continuous pasture (CP). And at two depths, in the superficial and sub-superficial layer, using volumetric rings and three repetitions were performed for each collection, totalizing 36 soil samples.

Figure 2 – Experimental map for the study area: (a) Piracaia, (b) Joanópolis and (c) Nazaré Paulista.


Source: Alexandre Uezu.

Figure 3 – Soil classes included in the study are Haplic Cambisol (CX), Regolith Neosol (RR), and Red Yellow Argisol (PVA).


Source: Author (2021).

Haplic Cambisol was found in Piracaia, Red Yellow Argisol was found in Joanopolis and Regolith Neosol in Nazare Paulista.

## 4.2 Determination of soil physical properties

### 4.2.1 Aggregates stability

Aggregate stability was measured using the methodology proposed by Yoder (1936) and described by Teixeira et al. (2017) with some modifications. Soil samples with preserved structure were collected at the sub superficial and superficial layer and then air-dried. All samples were pre-sieved to pass the opening of 7.93 mm and retained in the 4.75 mm, then weigh 25g of aggregates to obtain an aggregate sample. Following, a pre-treatment was done consisting of slow wetting, placing the sample on wet sand and protecting it with filter paper, then performing the analysis after 2 hours. When complete, the sample was transferred to the upper sieve of the sieving equipment in water and lasted for 15 minutes. Fractionation was done in six aggregate size classes (7.93-2, 2-1, 1-0.5, 0.5-0.25, 0.25-0.105, < 0.105 mm). After this operation, all the material from each sieve was transferred to a box previously identified and tared using a handle. They were allowed to settle and remove excess water, taking care not to lose any soil particles. Then they were dried in an oven at 105 – 110 °C for 48 hours and determined the weight of the aggregates in each size class, expressing it as a percentage of the initial sample, remembering that aggregates less than 0.105 mm will be passed through the water and must be determined by the difference. The WMD, GMD indices were calculated according to the method proposed by Kemper and Rosenau (1986), using equations 1 and 2, respectively.

$$WMD = \sum_{i=1}^{a} (x_i * w_i) \qquad \text{Eq. (1)}$$

where:

*WMD* = weighted mean diameter;

$x_i$ = average grade diameter (mm); and

$w_i$ = proportion of each class in relation to the total.

$$GMD = EXP \frac{\sum_{i=1}^{n} (w_i * \log x_i)}{\sum_{i=1}^{n} w_i} \qquad \text{Eq. (2)}$$

where:

*GMD* = geometric mean diameter;

$w_i$ = proportion of each class in relation to the total.

$x_i$ =average grade diameter (mm); and

$n$ = number of classes.

### 4.2.2 Textural analysis

For textural analysis using the pipette methodology (Day, 1965), 10 g of TFSA were placed in a bottle together with 10 mL of 1N NaOH and distilled water was added until the volume is complete. The material was agitated for 16 hours at 30 rpm on the Wagner agitator for the dispersion of the material.

Figure 4 – Soil texture analysis using the pipette method.

Source: Author (2021).

### 4.2.3 Bulk density (BD)

Following the core method, undisturbed soil samples were collected in metallic cylinders, which had their height and diameters previously measured. They were taken to an oven at 105 °C, weighed, emptied, and reweighed to determine the soil bulk density (Viana, 2009).

$$BD = \frac{W}{V} \qquad \text{Eq. (3)}$$

where:

*BD* = bulk density (g.cm$^{-3}$);

*W* = weight of the sample after being dried at 105 °C (g);

*V* = volume of the cylinder (cm$^{-3}$).

### 4.2.4 Total porosity

Total soil porosity was calculated using soil bulk density (*BD*), and particle density (PD) expressed as 2.65 mg.m$^{-3}$, the standard value for the equation (Silva *et al.*, 1994):

$$TP = \left[\frac{1 - BD}{PD}\right] \qquad \text{Eq. (4)}$$

where:
*TP* = total porosity ($cm^3$. $cm^3$);
*BD* = soil density (g. $cm^{-3}$);
*PD* = particle density.

### 4.2.5 Microporosity

Microporosity was determined using the tension table method (Embrapa 2007). It is initially placed with saturated samples on the tension table which eliminates the water from the macropores (pores of 0.05 mm diameter or greater). After being weighed before and after being dried in the oven at 105 °C and considering density of water equals to 1 g.$cm^{-3}$, the volume of micropores in the sample can be calculated as follows:

$$Micro = \frac{(a - b)}{c} \qquad \text{Eq. (5)}$$

where:
*Micro* = microporosity ($m^3$. $m^{-3}$);
*a* = dry soil mass + retained water, after equilibration with a potential of -6 kPa (g);
*b* = dry soil mass at 105 °C (g);
*V* = total sample volume in the cylinder ($cm^3$).

### 4.2.6 Macroporosity

Macroporosity refers to the volume of soil that corresponds to pores of 0.05 mm and can be calculated from the total porosity and microporosity values as follows:

$$Macro = (TP - Micro) \qquad \text{Eq. (6)}$$

where:
*Macro* = macroporosity ($m^3$. $m^{-3}$);
*TP* = total porosity ($m^3$. $m^{-3}$);
*Mi* = microporosity ($m^3$. $m^{-3}$).

## 4.3 Water infiltration

### 4.3.1 Data acquisition in field

Basic infiltration rate was performed using the methodology described in Bernardo *et al*. (2008), using the double ring infiltrometer method. The data was acquired in Red Yellow Argisols, Haplic Cambisols, and Regolith Neosols combined with land uses such as: native forest, eucalyptus, rotative and continuous pasture, three (3) repetitions was made under each land use (Figure 5). This instrument is composed of an ensemble of two concentric rings, the first ring being 20 cm and the second one being 40 cm in diameter. With a hammer, the two rings being introduced to a depth of 15 cm below the soil surface then a leveler to check if the rings were level. The first ring which has the role of reducing the lateral dispersion of the infiltrated water in the second ring, then infiltrating all along the soil profile in a vertical direction to avoid overestimating the infiltration rate. We also used a graduated ruler, then a plastic in the rings so that the water seeped into the two rings. The reading was made by the graduated ruler and the plastic was removed to start the reading. A chronometer was used to count the water infiltration time into the ground. When necessary, we put additional water to the rings.

Figure 5 – Double ring infiltrometer used in the soil water infiltration rate test.

Source: Author (2021).

### 4.3.2 Water infiltration models

Basic infiltration rate was estimated by empirical and theoretical models of Horton (1939), Kostiakov-Lewis, Philip (1957), and Kostiakov (1932).

#### 4.3.2.1 Horton model

Horton (1939) proposed an equation to determine the rate of infiltration of water into the soil which is as follows:

$$I = I_f + (I_i - I_f).e^{-c.t} \qquad \text{Eq. (7)}$$

where:
$I$ = instant infiltration rate (mm $h^{-1}$);
$I_f$ = constant/ stable final infiltration rate (mm $h^{-1}$);
$I_i$ = infiltration rate at the beginning of the experiment (mm $h^{-1}$);
$c$ = constant related to the format of the curve; and
$t$ = infiltration time (min).

#### 4.3.2.2 Kostiakov-Lewis model

This equation was developed to eliminate the deficiency of the infiltration rate to tend to zero when time tends to infinity.

$$I = k.T^{\alpha} + I_f\,.\,t \qquad \text{Eq. (8)}$$

where:
$I$ = infiltration (mm $h^{-1}$);
$k$ and $\alpha$ = constants that depend on the soil and its initial conditions, that is, they depend on the attributes of the soil, such as soil texture, moisture content, bulk density and other parameters;
$I_f$ = equilibrium (constant final infiltration rate); and
$t$ = time tending towards infinity (min).

#### 4.3.2.3 Philip model

Associated with the Darcy equation for unsaturated media and with the continuity equation one arrives at a second order partial non-linear differential equation, also called the Richards equation.

$$I = \frac{1}{2} S . t^{-1/2} + F \qquad \text{Eq. (9)}$$

where:
$I$ = infiltration (mm $h^{-1}$);
$S$ = constant determined by linear regression of infiltration as a function of $t^{-1/2}$;
$t$ = infiltration time (min); and
$F$ = gravity contribution constant for a ground movement.

#### 4.3.2.4 Kostiakov model

The empirical equation is based on the infiltration of the Kostiakov model developed in 1932, this one in the form of the connection of the field data curve.

$$I = k . t^{\alpha} \qquad \text{Eq. (10)}$$

where:
$I$ = infiltration (mm $h^{-1}$);
$k$ and $\alpha$ = constants that depend on the soil and its initial conditions, that is, they depend on the attributes of the soil, such as soil texture, moisture content, bulk density and other parameters; and
$t$ = time (min).

The determination of these parameters was carried out using the Excel software Solver tool, minimizing the error between the infiltration rate measured by Eq. (5) defined by:

$$Error = \sum (I_i - I_f)^2 \qquad \text{Eq. (11)}$$

where:

$I_i$ = observed values;

$I_f$ = estimated values.

### 4.4 Final water infiltration rate

In Table 1 below, according to Fonseca and Duarte (2006), final infiltration rate can be classified as very high, high, medium, and low. The final infiltration rate (FIR) was also determined using a potential equation (Kostiakov, 1932) which is as follows:

$$FIR = 60.a.n.T^{(n-1)} \quad \text{Eq. (12)}$$

where:

$a$ = constant dependent on the soil, varying between 0 and 1;

$n$ = parameter dependent on the condition of the initial soil moisture.

$T$ = time (min).

Table 1 – Classification Final Infiltration Rate (mm $h^{-1}$).

| Soils | mm.$h^{-1}$ |
|---|---|
| Very High | > 30 |
| High | 15 - 30 |
| Medium | 5 - 15 |
| Low | < 5 |

Source: Fonseca and Duarte (2006).

# 5 DATA ANALYSIS

Data collected in the field were entered and treated in Excel (2013). After this, descriptive statistics were calculated, considering that the study design was completely randomly determined. For statistical analysis, a principal component analysis (PCA) was performed to evaluate the soil properties and analysis of model performance data like coefficient of determination ($R^2$) and mean square error (MSE) were also used to determine the water infiltration rate by using the equations:

$$R^2 = \frac{[\sum_{i=1}^{n}(x_i - x) * y_i]^2}{\sum_{i=n}^{n}(x_i - x)^2 * \sum_{i=n}^{n}(y_i - y)^2} \quad \text{Eq. (13)}$$

$$MSE = \left[\frac{\sum_{i=0}^{N}(T_i - M_i)^2}{N}\right] * \frac{100}{M} \quad \text{Eq. (14)}$$

Analysis of variance (ANOVA) and the Tukey honest significant difference test (5%) the coefficient of variation (CV) was performed to compare the means of the infiltration rate. All statistical analyses were conducted using the RStudio for Statistical Computing together with the RStudio interface.

# 6 RESULTS AND DISCUSSION

## 6.1 Model performance

In the evaluation of the equations of these models, $R^2$ and error values correspond to desirable features. In general, Horton model presented higher $R^2$ (Table 2) and lesser error values (Table 3) for most of the soil types and land uses. In fact, the application of Horton model was performed to determine the water infiltration rate in the soil.

Table 2 - List of the models and adjustment ($R^2$) in the prediction of water infiltration rate for the soil classes combined with land uses.

| Soil Type | Model | $R^2$ values for each land use | | | |
|---|---|---|---|---|---|
| | | Continuous Pasture | Rotative Pasture | Native Forest | Eucalyptus |
| Regolith Neosol | Horton | 0.98 | 0.62 | 0.00 | 0.90 |
| | Kostiakov | 0.97 | 0.86 | 0.01 | 0.70 |
| | Kostiakov-Lewis | 0.96 | 0.86 | 0.00 | 0.95 |
| | Philip | 0.97 | 0.82 | 0.00 | 0.93 |
| Haplic Cambisol | Horton | 0.97 | 0.87 | 0.84 | 0.22 |
| | Kostiakov | 0.69 | 0.70 | 0.44 | 0.07 |
| | Kostiakov-Lewis | 0.69 | 0.70 | 0.44 | 0.01 |
| | Philip | 0.77 | 0.77 | 0.61 | 0.02 |
| Red Yellow Argisol | Horton | 0.49 | 0.79 | 0.19 | 0.69 |
| | Kostiakov | 0.51 | 0.81 | 0.01 | 0.41 |
| | Kostiakov-Lewis | 0.51 | 0.52 | 0.01 | 0.09 |
| | Philip | 0.60 | 0.67 | 0.02 | 0.17 |

Source: Author (2021).

Table 3 - List of models and errors values in the prediction of water infiltration rate for the soil classes combined with land uses.

| Soil Type | Model | Error values for each land use | | | |
|---|---|---|---|---|---|
| | | Continuous Pasture | Rotative Pasture | Native Forest | Eucalyptus |
| Regolith Neosol | Horton | -2.3 | -3.5 | 2.3 | -0.7 |
| | Kostiakov | 0.4 | 6.2 | 0 | 0 |
| | Kostiakov-Lewis | 0.4 | 6.2 | -268.2 | 0 |
| | Philip | 0.9 | 12.6 | -251.7 | 0 |
| Haplic Cambisol | Horton | -1.3 | 33.3 | 51.1 | 99 |
| | Kostiakov | -4.8 | 91.6 | -12.8 | 0 |
| | Kostiakov-Lewis | 9.2 | -120.3 | 1.2 | - 119.1 |
| | Philip | 17.9 | - 105.5 | 16.1 | - 103.3 |
| Red Yellow Argisol | Horton | - 0.2 | -14.5 | 0 | -0.2 |
| | Kostiakov | 4.1 | 1.6 | -53.4 | 0 |
| | Kostiakov-Lewis | 18.1 | 15.6 | -39.4 | -4.9 |
| | Philip | 26.7 | 24.4 | -27 | 12.1 |

Source: Author (2021).

## 6.2 Modeling the soil water infiltration curve

In the three soil classes studied combined with different land uses, the soil water infiltration rate curves were determined by the Horton’s model (Table 4). With time, the infiltration rates decrease exponentially following the curves which are in the graphs below which describe the process of the initiation of the infiltration under each land use and the curves shows the different models for the soil water infiltration rate (Figures 6– 8).

Table 4 – Soil water infiltration rate in four land use classes from: Haplic Cambisol, Red Yellow Argisol, and Regolith Neosol (mm $h^{-1}$).

| Land Use | Soil Type | | |
|---|---|---|---|
| | Haplic Cambisol | Red Yellow Argisol | Regolith Neosol |
| Continuous Pasture | 59.68 d | 19.32 c | 12.95 c |
| Rotative Pasture | 304.22 c | 37.65 c | 126.57 b |
| Native Forest | 577.69 a | 303.19 b | 596.27 a |
| Eucalyptus | 501.67 b | 577.98 a | 132.67 b |
| F-test | 267.6 | 233.4 | 4321 |
| SMD | < 0.0001 | < 0.0001 | < 0.0001 |
| CV (%) | 39 | 52.51 | 54.69 |

Source: Author (2021).

The different letters next to the means for each land use class show significant differences between land use types, obtained using the Tukey test.
SMD = Significant Minimum Difference; CV = Coefficient of Variation.

Figure 6 – Water infiltration rate value curves as a function of time for Red Yellow Argisol in land uses.

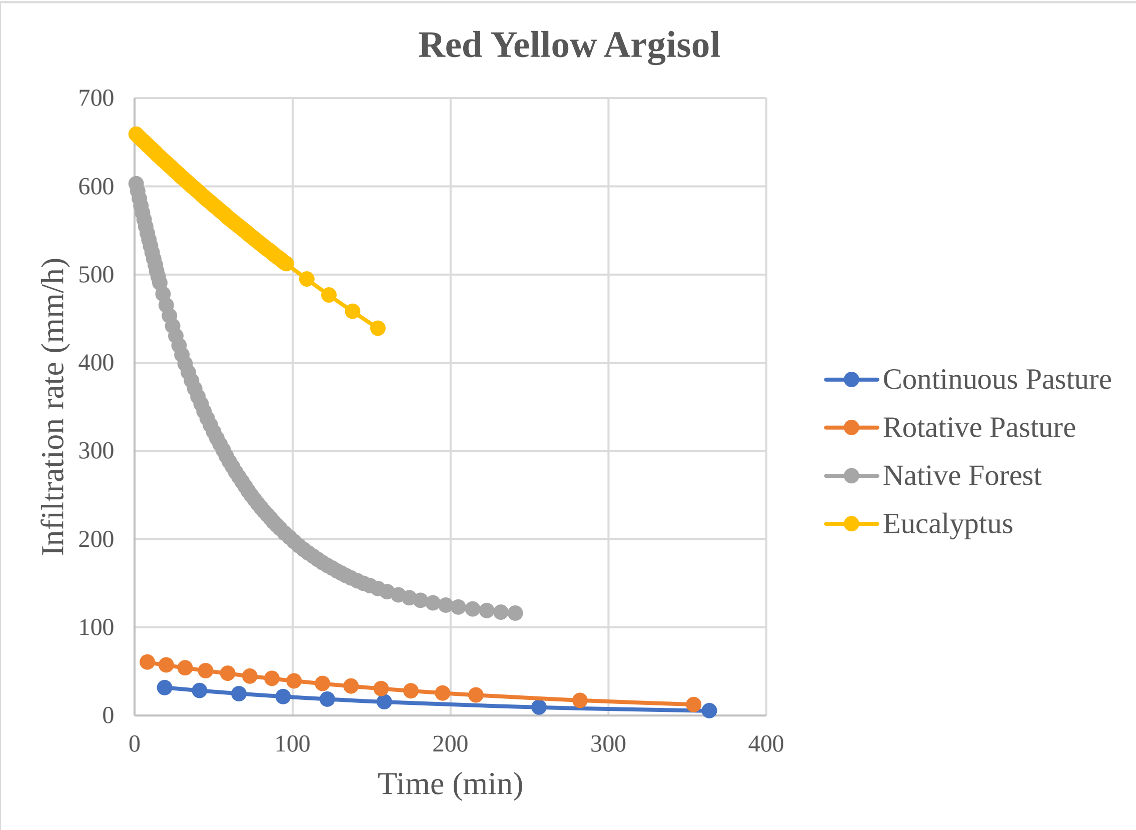


Source: Author (2021).

Figure 7- Water infiltration rate value curves as a function of time for Haplic Cambisol in land uses.

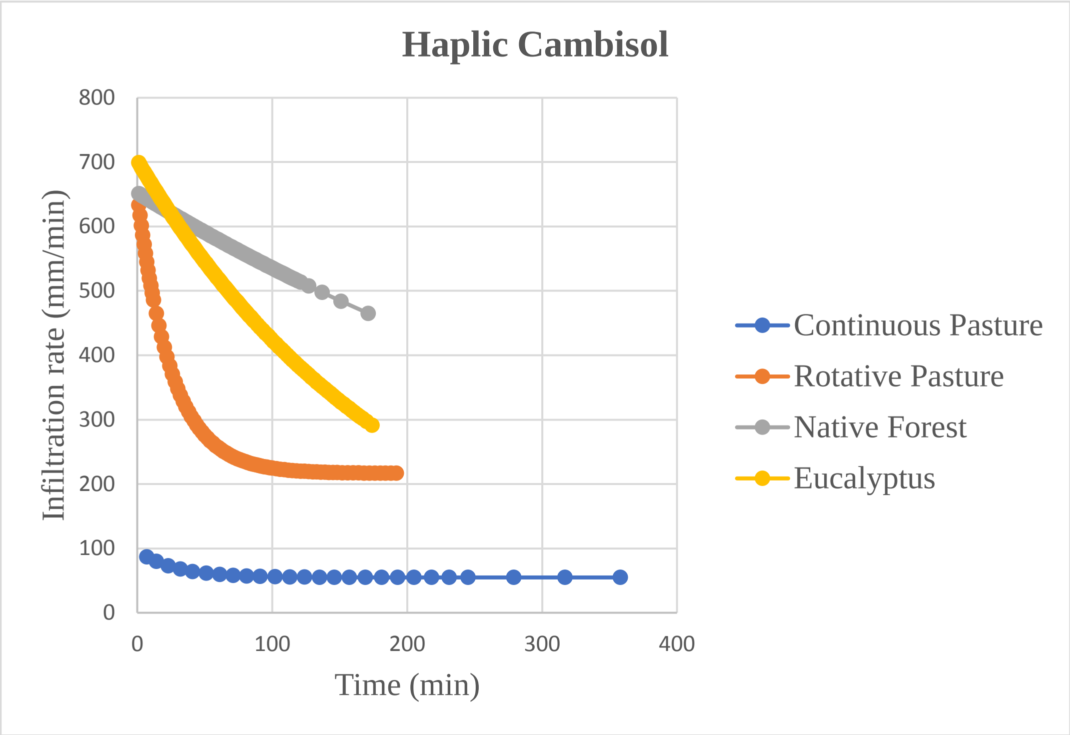


Source: Author (2021).

Figure 8 – Water infiltration rate value curves as a function of time for Regolith Neosol in land uses.

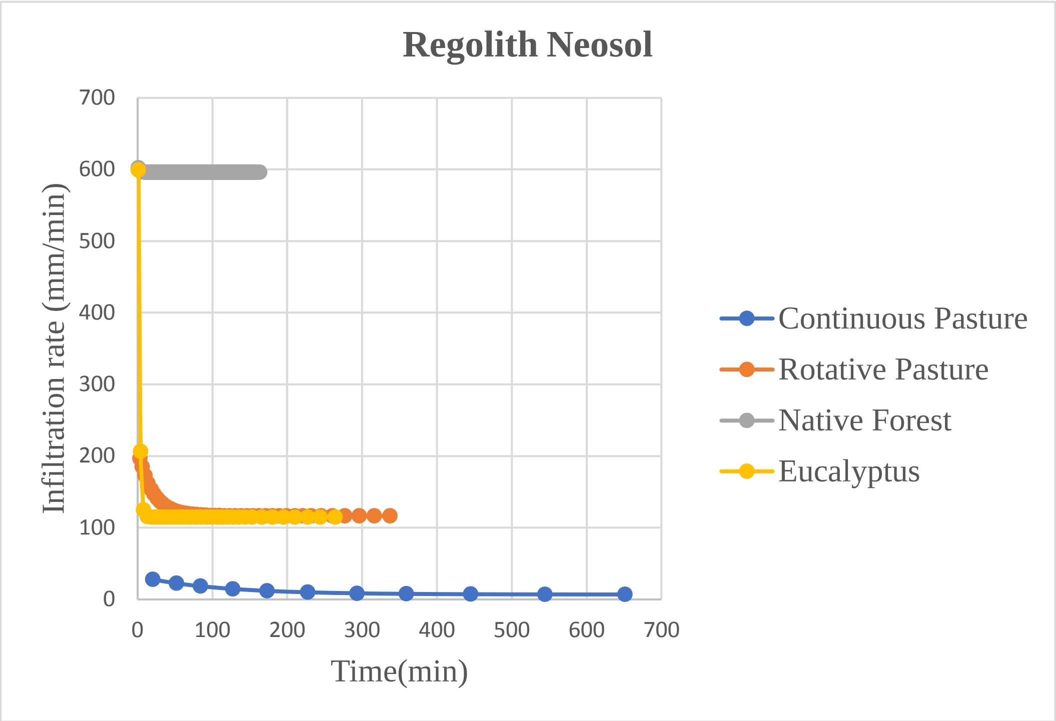


Source: Author (2021).

## 6.3 Basic infiltration rate of water into the soils

From the ANOVA analysis with Tukey HSD adjustment, it is clear that continuous pasture class is associated with the lowest soil water infiltration rate in each soil class. This result is similar to Lanzanova *et al*. (2010) observed that the water infiltration rate in the soil was altered by cattle trampling, and the water infiltration rate in the soil was altered as well when grazing had to carry out every 14 days. It should be noted that rotative pasture is not significantly different from continuous pasture in Red Yellow Argisol data and has the next lowest infiltration rate in the Haplic Cambisols and the Regolith Neosol.

The land use class with the highest observed infiltration rates differs across the soil classes, with native forest exhibiting the highest infiltration rate in Haplic Cambisol and Regolith Neosol, but eucalyptus showing the highest infiltration rate in Red Yellow Argisol. According to Carpanezzi (2000) eucalyptus in relation to other treatments like no-tillage and pasture can be explained by the fact that forests allow higher infiltration in the soil and subsoil, thus the soil becomes less prone to erosion, and more conserved given that the Red Yellow Argisol have a good aggregate stability and a much higher clay content than the other two soil classes.

Additionally, eucalyptus may have similar characteristics to native forest in terms of protection of the soil from water and erosion, given that eucalyptus is a managed forest landscape. This could explain why soil water infiltration rates are similar between eucalyptus and native forest, but much higher overall for continuous pasture and rotative pasture.

Under native forest land use in Haplic Cambisol and Regolith Neosol, the basic infiltration rate is respectively 465.5 mm.h$^{-1}$ and 596.16 mm h$^{-1}$ which is considered very high. NF may be associated with the variety of plant species present in forests, macropores, different root systems, and the presence of macrofauna in these soils. This result disagrees to the findings of Marcatto and Silva (2015), who found final water infiltration rates in the soil ranging from 2100 to 1560 mm h$^{-1}$ in the Pirapó River basin in the state of Paraná. Native forest has often been used as a comparison parameter, because of its greater conservation of physical and water properties of soils.

However, under eucalyptus area, the final infiltration rate of water into Red Yellow Argisol presented an infiltration rate of 439.19 mm h$^{-1}$ and higher than the other land use. This result could explain like areas with eucalyptus plantations allow improvements, maybe good concentrations of organic matter, as well as the large amounts of roots present that promote the approximation of particles, through the constant absorption of water in the soil profile.

According to Prevedello (2012), eucalyptus forest systems contribute to the improvement of structural quality, as they favor the formation of continuous pores, important for adequate aeration, retention and water conduction.

Considering the Regolith Neosol and Red Yellow Argisol under continuous pastureland use, the final infiltration rate of water (FIR) is considered “average” given their consecutive values of 5.34 mm $h^{-1}$ and 6.88 mm $h^{-1}$. This result is due to alterations in their physical structures such as soil compaction by animals trampling.

## 6.4 Assessment of soil physical properties

Table 5 contains the means and standard deviations of soil property variables for superficial and sub superficial layer of three soil classes, namely Haplic Cambisols (CX), Red Yellow Argisols (PVA), and Regolith Neosols (RR), and four different land use classes, namely Native Forest, Eucalyptus, Rotated Pasture, and Continuous Pasture. The soil properties being measured include geometric mean diameter, weighted mean diameter, bulk density, macroporosity, microporosity, total porosity, percent clay content, percent silt content and percent sand content. There are no standard deviation values for the three texture components in the Regolith Neosols data, due to only one sample was collected for each of the land use and horizons for this soil class. The table reveals that these soil parameters differ markedly across land use type, soil type, and horizon.

Table 5 – Mean and Standard Deviation (SD) of physical attributes of the soils corresponding to the uses: Native Forest (NF), Eucalyptus (E), Continuous Pasture (CP) and Rotative Pasture (RP) (to be continued).

| Attribute | Soil | Horizon | Use | | | | | | | |
|---|---|---|---|---|---|---|---|---|---|---|
| | | | Native Forest | | Eucalyptus | | Rotated Pasture | | Continuous Pasture | |
| | | | Mean | SD | Mean | SD | Mean | SD | Mean | SD |
| GMD | CX | A | 4.40 | 0.28 | 4.34 | 0.13 | 4.70 | 0.22 | 4.71 | 0.11 |
| | | B | 4.14 | 0.12 | 4.50 | 0.02 | 4.52 | 0.19 | 4.50 | 0.17 |
| | PVA | A | 4.48 | 0.33 | 4.84 | 0.06 | 4.46 | 0.04 | 4.73 | 0.25 |
| | | B | 3.31 | 0.66 | 3.64 | 0.07 | 1.97 | 0.18 | 4.63 | 0.22 |
| | RR | A | 4.37 | 0.18 | 4.53 | 0.15 | 4.46 | 0.78 | 4.76 | 0.16 |
| | | C | 4.62 | 0.30 | 4.64 | 0.29 | 4.82 | 0.09 | 4.80 | 0.30 |
| WMD | CX | A | 4.74 | 0.15 | 4.71 | 0.10 | 4.89 | 0.07 | 4.89 | 0.06 |
| | | B | 4.64 | 0.07 | 4.82 | 0.02 | 4.80 | 0.06 | 4.79 | 0.08 |
| | PVA | A | 4.80 | 0.13 | 4.94 | 0.02 | 4.79 | 0.01 | 4.90 | 0.08 |
| | | B | 4.18 | 0.43 | 4.30 | 0.03 | 3.26 | 0.19 | 4.84 | 0.10 |
| | RR | A | 4.22 | 0.46 | 4.32 | 0.50 | 4.29 | 1.04 | 4.70 | 0.30 |
| | | C | 4.58 | 0.20 | 4.85 | 0.04 | 4.68 | 0.27 | 4.65 | 0.61 |
| Bd | CX | A | 0.88 | 0.02 | 1.19 | 0.09 | 1.31 | 0.05 | 1.45 | 0.06 |
| | | B | 1.22 | 0.09 | 1.48 | 0.02 | 1.40 | 0.10 | 1.52 | 0.04 |
| | PVA | A | 1.14 | 0.12 | 1.26 | 0.04 | 1.32 | 0.12 | 1.44 | 0.06 |
| | | B | 1.59 | 0.06 | 1.39 | 0.03 | 1.58 | 0.04 | 1.52 | 0.06 |
| | RR | A | 0.66 | 0.03 | 0.77 | 0.17 | 0.87 | 0.04 | 0.96 | 0.01 |
| | | C | 1.11 | 0.07 | 1.21 | 0.06 | 1.25 | 0.06 | 1.27 | 0.21 |

Source: Author (2021).

Table 5 – Mean and Standard Deviation (SD) of physical attributes of the soils corresponding to the uses: Native Forest (NF), Eucalyptus (E), Continuous Pasture (CP) and Rotative Pasture (RP) (to be continued).

| Attribute | Soil | Horizon | Use | | | | | | | |
|---|---|---|---|---|---|---|---|---|---|---|
| | | | Native Forest | | Eucalyptus | | Rotated Pasture | | Continuous Pasture | |
| | | | Mean | SD | Mean | SD | Mean | SD | Mean | SD |
| Macro | CX | A | 0.17 | 0.06 | 0.18 | 0.06 | 0.09 | 0.02 | 0.09 | 0.02 |
| | | B | 0.16 | 0.03 | 0.11 | 0.05 | 0.14 | 0.03 | 0.13 | 0.02 |
| | PVA | A | 0.15 | 0.09 | 0.17 | 0.05 | 0.15 | 0.02 | 0.12 | 0.02 |
| | | B | 0.07 | 0.01 | 0.14 | 0.02 | 0.10 | 0.04 | 0.08 | 0.05 |
| | RR | A | 0.24 | 0.07 | 0.18 | 0.05 | 0.25 | 0.02 | 0.19 | 0.02 |
| | | C | 0.21 | 0.01 | 0.19 | 0.04 | 0.29 | 0.18 | 0.24 | 0.05 |
| Micro | CX | A | 0.29 | 0.03 | 0.31 | 0.03 | 0.39 | 0.03 | 0.37 | 0.01 |
| | | B | 0.40 | 0.02 | 0.36 | 0.04 | 0.37 | 0.03 | 0.34 | 0.02 |
| | PVA | A | 0.36 | 0.03 | 0.33 | 0.01 | 0.36 | 0.05 | 0.39 | 0.03 |
| | | B | 0.41 | 0.02 | 0.34 | 0.01 | 0.37 | 0.02 | 0.37 | 0.02 |
| | RR | A | 0.37 | 0.03 | 0.46 | 0.08 | 0.41 | 0.01 | 0.48 | 0.02 |
| | | C | 0.35 | 0.05 | 0.34 | 0.05 | 0.34 | 0.01 | 0.27 | 0.12 |
| TP | CX | A | 0.46 | 0.07 | 0.49 | 0.04 | 0.48 | 0.03 | 0.46 | 0.02 |
| | | B | 0.56 | 0.02 | 0.46 | 0.02 | 0.51 | 0.01 | 0.47 | 0.03 |
| | PVA | A | 0.51 | 0.09 | 0.50 | 0.06 | 0.51 | 0.04 | 0.51 | 0.04 |
| | | B | 0.47 | 0.02 | 0.48 | 0.02 | 0.47 | 0.06 | 0.45 | 0.03 |
| | RR | A | 0.62 | 0.08 | 0.65 | 0.05 | 0.66 | 0.02 | 0.67 | 0.03 |
| | | C | 0.56 | 0.03 | 0.53 | 0.02 | 0.63 | 0.19 | 0.52 | 0.11 |

Source: Author (2021).

Table 5 – Mean and Standard deviation (SD) of physical attributes of the soils corresponding to the uses: Native Forest (NF), Eucalyptus (E), Continuous Pasture (CP) and Rotative Pasture (RP) (concluded).

| Attribute | Soil | Horizon | Use | | | | | | | |
|---|---|---|---|---|---|---|---|---|---|---|
| | | | Native Forest | | Eucalyptus | | Rotated Pasture | | Continuous Pasture | |
| | | | Mean | SD | Mean | SD | Mean | SD | Mean | SD |
| %Clay | CX | A | 36.35 | 0.55 | 33.01 | 1.15 | 39.86 | 0.50 | 25.47 | 0.90 |
| | | B | 41.50 | 1.76 | 43.42 | 0.61 | 45.88 | 0.27 | 28.19 | 0.68 |
| | PVA | A | 37.76 | 0.27 | 33.54 | 1.65 | 23.01 | 1.64 | 25.47 | 0.90 |
| | | B | 44.48 | 0.53 | 56.04 | 0.50 | 39.58 | 2.89 | 26.09 | 0.68 |
| | RR | A | 54.95 | N/A | 38.04 | N/A | 42.27 | N/A | 55.47 | N/A |
| | | C | 28.81 | N/A | 45.05 | N/A | 44.00 | N/A | 26.72 | N/A |
| %Sand | CX | A | 49.14 | 2.74 | 52.83 | 4.08 | 43.51 | 1.03 | 47.53 | 1.92 |
| | | B | 38.98 | 2.18 | 44.48 | 0.51 | 40.24 | 1.10 | 42.03 | 0.40 |
| | PVA | A | 40.07 | 3.97 | 48.61 | 1.77 | 61.05 | 1.57 | 62.06 | 2.96 |
| | | B | 37.54 | 0.77 | 28.78 | 1.10 | 47.53 | 1.87 | 57.30 | 1.19 |
| | RR | A | 33.18 | N/A | 38.67 | N/A | 41.53 | N/A | 31.59 | N/A |
| | | C | 51.55 | N/A | 23.05 | N/A | 33.53 | N/A | 55.74 | N/A |
| %Silt | CX | A | 14.51 | 3.29 | 14.16 | 2.98 | 16.62 | 0.65 | 18.76 | 1.59 |
| | | B | 19.52 | 2.64 | 12.09 | 1.10 | 13.88 | 0.86 | 16.12 | 1.19 |
| | PVA | A | 22.18 | 4.20 | 17.85 | 1.01 | 15.95 | 2.25 | 12.48 | 2.52 |
| | | B | 17.98 | 1.09 | 15.18 | 1.04 | 12.89 | 3.81 | 14.51 | 0.75 |
| | RR | A | 11.88 | N/A | 23.29 | N/A | 16.21 | N/A | 12.93 | N/A |
| | | C | 19.64 | N/A | 31.90 | N/A | 22.47 | N/A | 17.54 | N/A |

Source: Author (2021).

The soil properties of sub superficial and superficial layers were correlated using Correlation matrix and Principal Components Analysis (PCA) methods associated with final water infiltration rate under the land uses (Figure 9 to 11).

Figure 9 – Correlation matrix of soil properties (Horizon A and B) associated to basic infiltration rate of water.

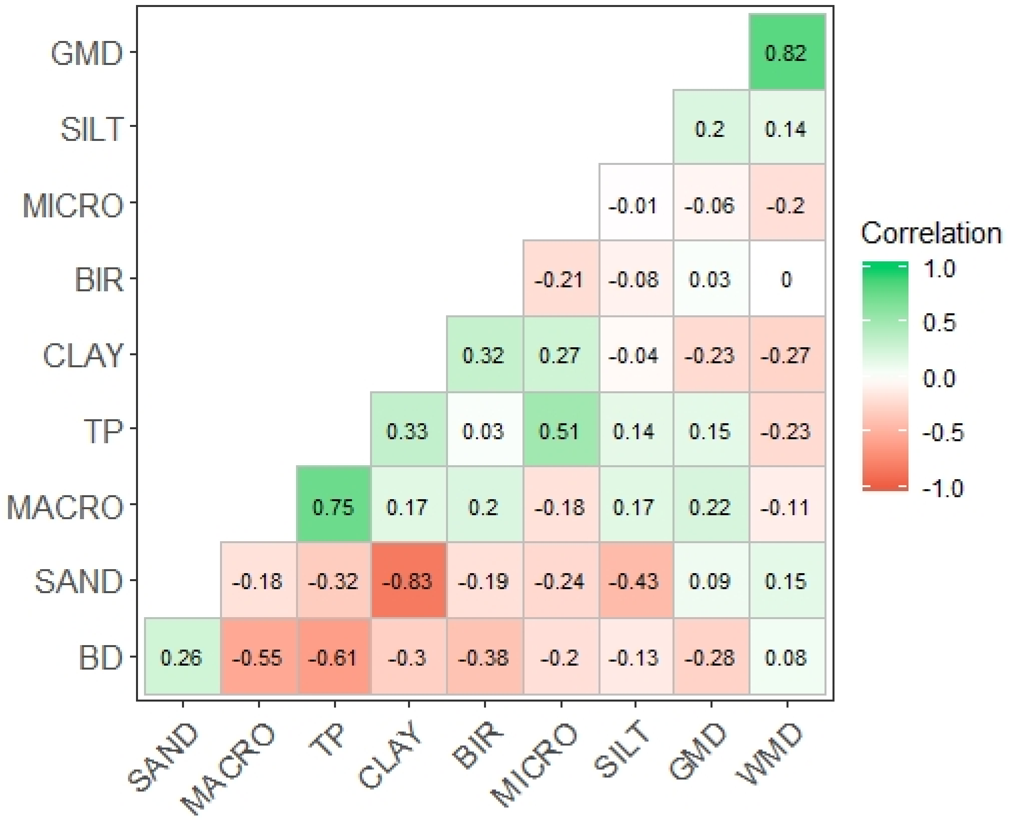


Source: Author (2021).

Clay and macroporosity have positive linear correlation of 0.32 and 0.2 respectively to BIR. These results explain soils with higher percentage of clay and macro, higher their basic infiltration rate of water under the land use. However, Silt, microporosity, Bulk density, sandy and Basic infiltration rate have negative linear correlation of -0.08, -0.21, -0.38, -0.19, respectively. These results explain that as one these soil properties variables increased, Basic infiltration rate of water (BIR) under the land use decreased. Therefore, these variables seem to measure the same characteristic. There is no significant correlation occurs between GMD, WMD and basic infiltration rate of water (BIR).

Figure 10 – Principal component analysis method of soils properties and Basic Infiltration Rate of water with land uses.

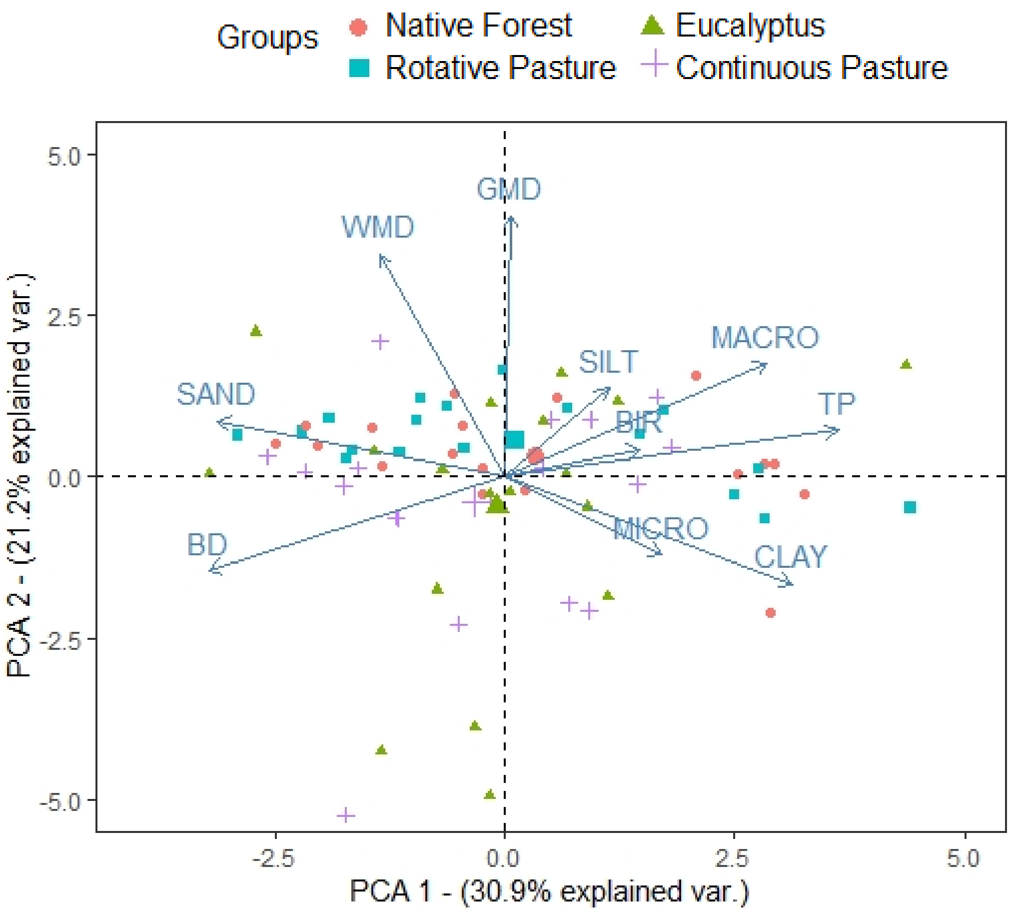


Source: Author (2021).

Figure 9 shows that BIR tends to increase in areas with higher Macro, TP, Clay which are in areas with native forest (NF) and rotation pasture (RP). BIR tends to decrease in areas with higher silt, micro, BD, sand with continuous and also rotative pasture. WMD, GMD are not significative to BIR.

Figure 10 shows that BIR tends to increase in areas with higher Macro, Total Porosity, Clay which are in soil type CX and RR. BIR tends to decrease in areas with higher silt, micro, Bulk density, sand with RR. WMD, GMD are not significative to BIR.

Figure 11 – Principal component analysis method of soils properties and Basic Infiltration Rate of water with soil classes.

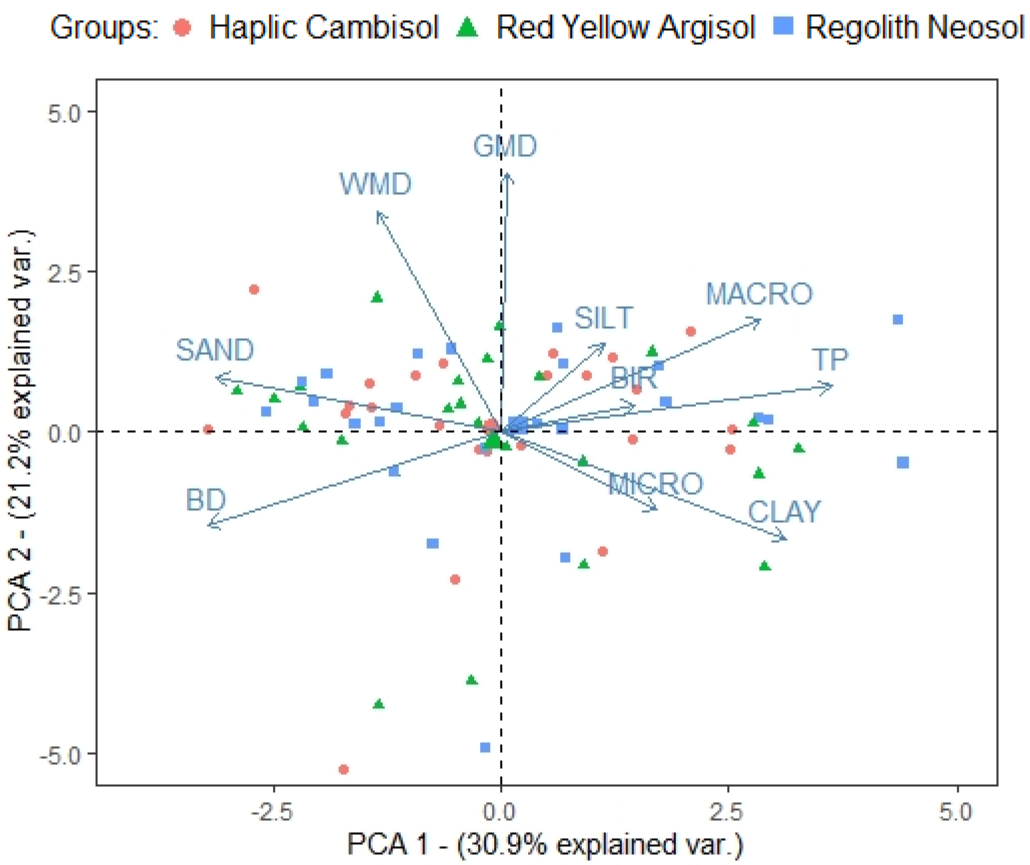


Source: Author (2021).

# 7 CONCLUSIONS

In general, Cambisols, Red Yellow Argisols and Neosols under the native forest and eucalyptus represented higher important areas for preservation that will influence the recharge of water in the soil.

Water infiltration correlated with increased macroporosity and lower bulk density.

The basic infiltration rate in Red Yellow Argisols under the eucalyptus land cover is higher than the other land use types such as pasture in rotation, and continuous pasture.

Native forest and eucalyptus presented better rate of infiltration compared to the continuous and rotative pastures.

# REFERENCES

AGÊNCIA NACIONAL DE ÁGUAS (ANA). Conjuntura dos recursos hídricos no Brasil: encarte especial sobre a crise hídrica. Brasil: ANA. Disponível em: <Available on: http://conjuntura.ana.gov.br/docs/crisehidrica.pdf >. Acessed in 10 august of 2016. 2014.

ALMEIDA, C. L.; OLIVEIRA, J. G. B.; ARAUJO, J. C. Impacto da recuperação de área degradada sobre as respostas hidrológicas e sedimentológicas em ambiente semiárido. Water Resources and Irrigation Management, v.1, n.1, pp. 39-50, 2012.

ALMEIDA, A. Q. DE et al. Modeling of Water Infiltration in Soil Cultivated With Eucalyptus and Pasture. Revista Caatinga, v. 27, n. 1, pp. 148-153, 2014.

ALVES, M. C.; CABEDA, M. S. V. Influência da água em um Podzólico Vermelho-escuro sob dois métodos de preparo, usando chuva simulada com duas intensidades. Revista Brasileira de Ciência do Solo, Viçosa. v. 23, n. 4, pp. 735-761, 1999.

ALVES SOBRINHO, T.; VITORINO, A. C. T.; SOUZA, L. C. F.; GONÇALVES, M. C.; CARVALHO, D. F. Infiltração de água no solo em sistemas de plantio direto e convencional, 2003.

ANACHE, J. A. A.; FLANAGAN, D. C.; SRIVASTAVA, A.; and WENDLAND, E. C. Land use and climate change impacts on runoff and soil erosion at the hillslope scale in the Brazilian Cerrado. Sci Total Environ, pp. 622-623, p. 140-151, 2018.

ARAÚJO NETO, J. R.; ANDRADE, E. M.; PALÁCIO, H. A. Q.; SANTOS, J. C. N.; LOBATO, F. A. O. Análise comparativa do escoamento superficial de microbacias experimentais em clima semiárido tropical. Water Resources and Irrigation Management, v. 2, n. 3, pp. 111-120, 2013.

ARNOLD, J. G.; MUTTIAH, R. S.; SRINIVASAN, R.; ALLEN, P. M. Regional estimation of base flow and groundwater recharge in the upper Mississippi river basin. Journal of Hydrology 227; pp. 21-40, 2000.

ATLAS DOS SERVIÇOS AMBIENTAIS DO SISTEMA CANTAREIRA - 1. ed. - São Paulo: Memnon Edições Científicas: IPÊ - Instituto de Pesquisas Ecológicas, 2017.

BERNARDO, S.; SOARES, A. A.; MANTOVANI, E. C. Manual de irrigação. 8. Viçosa: UFV, 625 p., 2006.

BERNARDO, S.; SOARES, A. A.; MANTOVANI, E. C. Manual de irrigação. 8. Viçosa: UFV, 625 p., 2008.

BONO, J. A. M.; et al. Infiltração de água no solo em um latossolo vermelho da região sudoeste dos cerrados com diferentes sistemas de uso e manejo. Revista Brasileira de Ciência do Solo, Campinas, v.36, pp. 1845-1853, 2012.

BRANDÃO, V. S.; SILVA, D. D.; RUIZ, H. A.; PRUSKI, F. F.; SCHAEFER, C. E. G. R.; MARTINEZ, M. A.; MENEZES, S. J. M. C. Resistência hidráulica da crosta formada em solos submetidos a chuvas simuladas. Revista Brasileira de Ciência do Solo, Viçosa, v.30, pp. 13-22, 2006.

CAPENEZZI, A. A. Benefícios Indiretos da Floresta. In: GALVÃO, A. C. M. Ed. Reflorestamento de Propriedades Rurais para fins Produtivos e Ambientais: Um guia para ações municipais e regionais. Colombo, PR: Embrapa Florestas, pp. 19-56, 2000.

CARVALHO, D. F.; and SILVA, L. D. B. Hidrologia: Infiltração. Rio de Janeiro. UFRRJ, 21 p., 2006.

CECILIO, R. A.; SILVA, D. D.; PRUSKI, F. F.; MARTINEZ, M. A. Modelagem da infiltração de agua no solo sob condições de estratificação utilizando-se a equação de Green-Ampt. Revista Brasileira de Engenharia Agrícola e Ambiental 7 (3): 415- 422, 2003.

DAY, P.R. Particle fractionation and particle size analysis. In: BLACK, C.A.; ed. Methods of soil analysis; physical and mineralogical properties including statistics of measurement and sampling. Madison, American Society of Agronomy, 1965. pt. l, p.545-67.

DIDONÉ, E. J., MINELLA, J. P. G., and MERTEN, G. H. Quantifying soil erosion and sediment yield in a catchment in southern Brazil and implications for land conservation. J Soils Sediments, 15 (11), pp. 2334-2346, 2015.

DIODATO, N.; CECARRELI, M. Computational uncertainty analysis of groundwater recharge in catchment. Ecological informatics 1(4): 377-389, 2006.

EMBRAPA - Empresa Brasileira de Pesquisa Agropecuária - Centro Nacional de Pesquisa de Solos. Manual e Métodos de análise de solos. Rio de Janeiro, Embrapa Solos, 212p., 2007.

ESPINDOLA, J. A. A.; et al. Estratégias para utilização de leguminosas para adubação verde em unidades de produção agroecológica. Documentos 174. Embrapa Agrobiologia, Seropédica, RJ, 24 p., 2004.

FONSECA, F.C; and DUARTE, L. B. Hidrologia. Capitulo 5. Infiltração, agosto, 2006.

FREITAS, P. L. Contribuição do uso da terra e do manejo do solo para a recarga de aquifer. Rio de Janeiro: Ministerio da Agricultura, Pecuária e Abastecimento. 4 p., Technical communication, 32, 2005.

FREITAS, D. A. F.; OLIVEIRA, A. H.; SILVA, M. L. N.; LIMA, G. C.; GOMIDE, P. H. O.; PEREIRA, P. H.; SANTOS, D. G.; VEIGA, F. Aptidão agrícola das terras na sub- bacia das posses, no município de Extrema, Região Sup do Estado de Minas Gerais. In: Congresso de Pós-graduação da UFLA, I Encontro de Engenharia de Sistemas e IV Workshop de Laser e Óptica na Agricultura, 17, Lavras: UFLA, 2008.

GASPAR, M. T. P.; CAMPOS, J. E. G.; CADAMURO, A. L. M. Condições de infiltracao em solos na região de recarga do sistema aquiferp Urucuia no oeste da Bahia sob diferentes condições de uso. Revista Brasileira de Geociências 37(3): 542-550, 2007.

GONDIM, T. M. S.; WANDERLEY, J. A. C.; SOUZA, J. M.; FEITOSA FILHO, J. C.; SOUSA, J. S. Infiltração e velocidade de infiltração de água pelo método do infiltrômetro de anel em solo areno-argiloso. Revista Brasileira de Gestão Ambiental, (Pombal – PB – Brasil) v. 4, n. 1, pp. 64-73, 2010.

GUERRA, H. C. Física dos solos. Campina Grande: UFPB, 175 p., 2000.

HORTON, R. E. Analysis of runoff plat experiments with varying infiltration capacity Trans. Am. Geophys. Union 20, pp. 693-711, 1939.

IBGE. Manual Técnico de Uso da Terra. Instituto Brasileiro de Geografia e Estatística. 2ª ed. Rio de Janeiro: IBGE. 171 p., 2006.

JONES, I. C.; BANNER, J. L. Estimation recharge threshold in tropical karst island aquifers: Barbados, Puerto Rico, and Guam. Journal of Hydrology 278: 131-143, 2003.

KEESE, K. E.; SCANLON, B. R.; REEDEY, R. C. Assessing controls on diffuse groundwater recharge using unsaturated flow modeling. Water resources Research 41 (w06010): 1-12, 2005.

KOSTIAKOV, A.N. The Dynamics of the Coefficient of Water Percolation in Soils and the Necessity for Studying It from a Dynamic Point of View for Purpose of Amelioration. Society of Soil Science, 14, pp. 17-21, 1932.

LANZANOVA, M. E.; ELTZ, F. L. F.; NICOLOSO, R. S.; AMADO, T. F. C.; REINERT, D. J.; ROCHA, M. R. Atributos físicos de um Argissolo em sistemas de culturas de longa duração sob semeadura direta. Revista Brasileira de Ciência do Solo, Viçosa, v. 34, n.5, pp. 1333-1342, 2010.

LAWALL, S.; SANTOS, A. C. F.; MOTA, P. O.; FERNANDES, N. F. Modificações da dinâmica hidrológica do solo em resposta as mudanças de uso e cobertura: Um estudo de caso na região serrana do Rio de Janeiro. Anais... 12º Encontro de Geografos da América Latina, Montevidéo, Uruguai, pp. 7467-7477, 2009.

LUCAS-BORJA, M. E., CARRÀ, B. G.; NUNES, J. P.; BERNARD-JANNIN, L.; ZEMA, D. A., and ZIMBONE, S. M. Impacts of land-use and climate changes on surface runoff in a tropical forest watershed (Brazil). Hydrological sciences journal, 65 (11), pp. 1956-1973, 2020.

MARCATTO, F. S.; SILVEIRA, H. Avaliação físico-hídrica do Latossolo Vermelho textura argilosa: subsídios a gestão dos recursos hídricos na bacia hidrográfica do Pirapó-PR. Revista do Programa de PósGraduação em Geografia Maringá, 7(1): 117-138, 2015.

MARIOTI, J.; BERTOL. I., RAMOS, J. C.; WERNER, R. S.; PADILHA, J.; FLORES, M. C.; BANDEIRA, D.H. Erosão hídrica em semeadura direta de milho e soja nas direções da pendente e em contorno ao declive, comparada ao solo sem cultivo e descoberto. R Bras Ci Solo, 37:1361-71, 2013.

MAZURAK, A. P. Effect of gaseous phase on water-stable synthetic aggregates. Soil Sci. 69:135-148, 1950.

MELO, J. G.; STEIN, P.; VASCONCELOS, M. B.; SILVA, F. H. R. Recarga do aquífero Açuna borda Sudeste da bacia Pottiguai Trecho Apadi-Upanema. Revista de Geologia 19(4): 61-72, 2006.

MENEZES, M. D.; JUNQUEIRA JUNIOR, J. A.; MELLO, C. R.; SILVA, A. M.; CURI, N.; MARQUES, J. J. Dinâmica hidrológica de duas nascentes associadas ao uso do solo, características pedológicas e atributos físico-hídricos na sub- bacia hidrográfica do Ribeirão Lavrinha-Serra da Mantiqueira (M.G). Scientia Foretalis 37 (82): 175-184, 2009.

OKI, T.; KANAE, S. Global hydrological cycles and world water resources. Science, 313, pp. 1068-1072, 2006.

PHILIP, J. R. The theory of infiltration: 1. The infiltration equation and its solution. Soils Science. 83:345-357, 1957.

PINHEIRO, A.; TEIXEIRA, L. P.; KAUFMANN, V. Capacidade de infiltração de água em solos sob diferentes usos e práticas de manejo agrícola. Ambi-Agua, An Interdisciplinary Journal of Applied Science, v. 4, n. 2, pp. 188-199, 2009.

PREVEDELLO, C.L. Física do Solo com problemas resolvidos. Curitiba: C.L. Prevedello, 1996.

PREVEDELLO, J. Dinâmica do armazenamento e da disponibilidade de água em Argissolo sob eucalipto e campo nativo. 120 f. Tese (Doutorado em Engenharia Florestal) - Universidade Federal de Santa Maria. Centro de Ciências Rurais. Santa Maria. RS, 2012.

PRICE, K.; JACKSON, C. R.; PARKER, A. J. Variation of surficial soil hydraulic properties across land uses in the southern Blue Ridge Mountains, North Carolina, Journal of Hydrology, USA. v. 383, n. 3-4, pp. 256-268, 2010.

REICHARDT, K. Água em sistemas agrícolas. São Paulo: Manole, 188 p., 1987.

SAMPAIO, L. F.; OLIVEIRA, M. P. P.; CASSARO, R.; RODRIGUES, V. G. S.; PEJON, O. J.; SÍGOLO, J. B.; and FERREIRA, V. M. Gully erosion, land uses, water and soil dynamics: A case study of Nazareno (Minas Gerais, Brazil). Dyna rev.fac.nac. minas, 83(199), pp. 198-206, 2016.

SIHAG, P.; TIWARI, N. K.; RANJAN, S. Estimation and inter-comparison of infiltration 32 models. Water Science, v. 31, n. 1, p. 34–43, 2017.

SILVA, A. P.; KAY, B. D.; and PERFECT, E. Characterization of the least limiting water range. Soil Sci. Soc. Am. J., 58:1775-1781, 1994.

SILVA, E. P. F. Velocidade de infiltração em área pastagem degradada e floresta natural no município de Porto Velho (RO). Revista franco-brasileira de geografia-Confins, n. 29, 2016.

SILVA, S. R.; BARROS, N. F.; COSTA, L. M. Atributos Físicos de dois Latossolos Afetados pela Compactação do Solo. Revista Brasileira de Engenharia Agrícola e Ambiental. 10: 842-847, 2006.

SOARES, P. V.; PEREIRA, S. Y.; SIMÕES, S. J. C.; BERNARDES, G.P.; BARBOSA, S. A. Mapa de infiltração do Alto e Médio Vale do Paraíba do Sul com base em elementos do meio físico e da precipitação, Taubaté, v. 3, n. 1, pp. 26-42, 2008.

STÜRMER, S. L. K.; DALMOLIN, R. S. D.; AZEVEDO, A. C.; PEDRON, F. A.; and MENEZES, F. P. Relação da granulometria do solo e morfologia do saprolito com a infiltração de água em Neossolos Regolíticos do rebordo do Planalto do Rio Grande do Sul. Ci. Rural, 39:2057-2064, 2009.

TEIXEIRA, C. F. A.; DAME, R. C. F.; TERRA, V. S. S.; REISSER, J. C.; SIMONETE, M. A.; BRIXNER, G. F. Estimativa da infiltração de água através de modelos empíricos em um Argissolo Vermelho Amarelo sob cultivo de pessegueiro, cv Maciel, VIII Reunião Sul Brasileira de Ciência do Solo, Pelotas - RS, 2010.

TEIXEIRA et al. Manual de métodos de análise do solo. Embrapa, 3 ed. revisada e ampliada, Brasília, 2017.

VANACKER, V.; AMEIJEIRAS-MARIÑO, Y.; SCHOONEJANS, J.; CORNÉLIS, J. T.; MINELLA, J. P. G.; LAMOULINE, F.; VERMEIRE, M. L.; CAMPFORTS, B.; ROBINET, J.; VAN DE BROEK, M.; DELMELLE, P.; and OPFERGELT, S. Land use impacts on soil erosion and rejuvenation in Southern Brazil. Catena (Giessen), 178, pp. 256-266, 2019

VIANA, J. H. M. Determinação da densidade de solos e de horizontes cascalhentos. Sete Lagoas: Embrapa Milho e Sorgo, Embrapa Milho e Sorgo. Comunicado técnico, 154, 2009.

WHATELY, M.; and CUNHA, P. Cantareira 2006: Um olhar sobre o maior manancial de água da região metropolitana de São Paulo (A view on the Sao Paulo Metropolitan Region larger water source) (pp. 68). São Paulo: Instituto Socioambiental, 2007.

YODER, R. E. A direct method of aggregate analysis of soils and a study of the physical nature of erosion losses. Journal of the American Society of Agronomy, v. 28, n. 5, pp. 337-351, 1936.

# ANNEX A – Photos taken during the work field.

# ANNEX B - RStudio code

```
attach(Evans_dados_PCA_)

library(factoextra)

library(FactoMineR)

library(ggplot2)

library(ggcorrplot)

library(psych)

names(Evans_dados_PCA_) <- c("SOIL", "GMD", "WMD", "BD","MACRO", "MICRO", "TP", "CLAY", "SAND","SILT", "BIR")

Evans_dados_PCA_$SOIL <- factor(c(1,2,3), labels = c("CX", "PVA", "RR"))

dados <- Evans_dados_PCA_[, -1]

describe(dados)

boxplot(dados)

boxplot(scale(dados))

matcor <- round(cor(dados), 2)

ggcorrplot(matcor, hc.order = TRUE, type = "lower", lab = TRUE, lab_size = 3, method="square", colors = c("tomato2", "white", "springgreen3"), title=,legend.title = "Correlation",ggtheme=theme_test())

Bartlett.sphericity.test <- function(x)

method <- "Bartlett's test of sphericity"

data.name <- deparse(substitute(x))

x <- subset(x, complete.cases(x)) # Omit missing values

n <- nrow(x)

p <- ncol(x)

chisq <- (1-n+(2*p+5)/6)*log(det(cor(x)))
```

```
df <- p*(p-1)/2
p.value <- pchisq(chisq, df, lower.tail=FALSE)
names(chisq) <- "X-squared"
names(df) <- "df"
return(structure(list(statistic=chisq, parameter=df, p.value=p.value,
                 method=method, data.name=data.name), class="htest"))
}
Bartlett.sphericity.test(dados)
# PCA com a matriz de cor
res.pca.cor <- PCA(dados, scale.unit = T, graph = FALSE)
# matriz de covariância
round(cor(dados),4)
round(res.pca.cor$eig,3)
round(res.pca.cor$svd$V,3)
res.pca.cor$eig
fviz_screeplot(res.pca.cor, ncp=4)+ theme_minimal()
# A correlação entre uma variável e um CP é chamada de carga (loadings).
round(res.pca.cor$var$cor,4)
# banseando-se na matriz de cor
round(res.pca.cor$var$cor^2,4)
# Quanto mais próxima uma variável for do círculo de correlações, melhor sua representação no mapa fatorial (e mais importante é a variável para a interpretação desses componentes)
# As variáveis próximas ao centro do gráfico são menos importantes para os primeiros componentes.
```

# No gráfico abaixo os componentes são coloridas de acordo com os valores do coseno quadrado:

fviz_pca_var(res.pca.cor, col.var="cos2") +

scale_color_gradient2(low="white", mid="blue",

high="red", midpoint=0.5) + theme_minimal()

# Coordenadas de variáveis

round(res.pca.cor$var$coord,2)

# Cos2: é uma medida que indica a qualidade da representação para variáveis no mapa fatorial

round(res.pca.cor$var$cos2,2)

# A contribuição das variáveis pode ser extraída da seguinte forma:

round(res.pca.cor$var$contrib,2)

# veja que a soma é igual a 100%

sum (res.pca.cor$var$contrib[,1])

# Quanto maior o valor da contribuição, mais a variável contribui para o componente.

# As variáveis mais importantes associadas a um determinado PC podem ser visualizadas, usando a função fviz_contrib () [factoextra package], da seguinte forma:

# Contribuições de variáveis no PC1

fviz_contrib(res.pca.cor, choice = "var", axes = 1)+ theme_minimal()

# Contribuições de variáveis no PC2

fviz_contrib(res.pca.cor, choice = "var", axes = 2)+ theme_minimal()

# Contribuição total nos PC1 e PC2

fviz_contrib(res.pca.cor, choice = "var", axes = 1:2)+ theme_minimal()

# Controle as cores das variáveis usando suas contribuições

# a cor representa a contribuição conjunta dim1-dim2

fviz_pca_var(res.pca.cor, col.var="contrib")+ theme_minimal()

```
# Alterar a cor
fviz_pca_var(res.pca.cor, col.var="contrib") + scale_color_gradient2(low="white", mid="blue",
            high="red", midpoint=2.5) + theme_minimal()
res.desc <- dimdesc(res.pca.cor, axes = c(1,2))
# Descrição da dimensão 1
res.desc$Dim.1
# Descrição da dimensão 2
res.desc$Dim.2
# Descrição da dimensão 3
res.desc$Dim.3
# Gráfico de escores (indivíduos ou pontos objetos)
# As coordenadas dos escores nos componentes principais são:
round(res.pca.cor$ind$coord,2)
fviz_pca_ind(res.pca.cor)+ theme_minimal()
#Cos2: qualidade da representação para escores nos componentes principais
# O coseno quadrado mostra a importância de um componente para uma determinada observação.
round(res.pca.cor$ind$cos2,3)
fviz_pca_ind(res.pca.cor, col.ind="cos2") +
  scale_color_gradient2(low="white", mid="blue",
            high="red", midpoint=0.50) + theme_minimal()
# Contribuição dos escores para os componentes principais
round(res.pca.cor$ind$contrib,2)
# Contribuições de escores para PC1
```

```
fviz_contrib(res.pca.cor, choice = "ind", axes = 1)+ theme_minimal()

# Contribuições de escores para PC2

fviz_contrib(res.pca.cor, choice = "ind", axes = 2)+ theme_minimal()

# Contribuição total em PC1 e PC2

fviz_contrib(res.pca.cor, choice = "ind", axes = 1:2)+ theme_minimal()

# Contribuições dos escores para PC1  (apenas os "top")

fviz_contrib(res.pca.cor, choice = "ind", axes = 1:2, top = 5)+ theme_minimal()

# Mundando a cor

fviz_pca_ind(res.pca.cor, col.ind="contrib") +
  scale_color_gradient2(low="white", mid="blue",
                      high="red", midpoint=50) + theme_minimal()

fviz_pca_biplot(res.pca.cor)+ theme_minimal()

fviz_pca_biplot(res.pca.cor, xlim =c(-4,5),ylim =c(-4,4),xlab ="PCA 1 - (33.6% explained var.)", geom.ind = "point", ylab ="PCA 2 - (23.1% explained var.)" ,title ="", habillage=(Evans_dados_PCA_$SOIL)) + theme_test() + theme(legend.position = "top")
```